NUMERICAL STUDIES ON FIRE ENVIRONMENT BY A FIELD MODEL

G.W. Zou
Department of Building Engineering, Harbin Engineering University, Harbin, Heilongjiang, China

W.K. Chow
Department of Building Services Engineering, The Hong Kong Polytechnic University, Hong Kong, China

(Received 23 July 2003; Accepted 20 August 2003)

ABSTRACT

Indoor environment in a compartment fire will be simulated by the field model Fire Dynamics Simulator FDS version 3.01. Theory behind this model is briefly reviewed first. Numerical experiments are then carried out in a compartment of size similar to the standard room-corner fire tests but with liquid pool fires. Results are compared with full-scale burning tests reported earlier in a new full-scale burning facility, the PolyU/HEU Assembly Calorimeter. It is observed that fairly accurate results can be predicted by FDS. However, the predicted results are sensitive to initial temperature as demonstrated by this study.

1. INTRODUCTION

With the rapid development of computer hardware, it is possible to use building fire field models [e.g. 1], also known as application of Computational Fluid Dynamics (CFD) or Numerical Heat Transfer (NHT), for fire safety designs [e.g. 2]. This happens frequently while implementing fire safety engineering approach for passive building construction for fire protection in Hong Kong [3] since 1998. In studying fire-induced convective flow by CFD/NHT, at least three parts have to be considered.

- Turbulence.
- Discretization of the set of partial differential equations with the convective term.
- Velocity-pressure linked equations.

Most of the CFD/NHT software were developed with turbulence treated by the Reynolds Averaging Navier-Stokes Equations (RANS) [e.g. 1,4,5] method. There are many good reasons for using RANS as the computing efforts (both core memory and processing time) are affordable by smaller consulting companies. However, there are many adjustable empirical parameters in the turbulent models concerned. Further, problems on dealing with relaxation and convergence criteria, false diffusion and sudden changes of thermal power in regions adjacent to the fire might be encountered. Many trial runs have to be carried out to get 'converged' results.

Based on years of research, the Fire Dynamics Simulator 3.01 (FDS) [6,7] was released by the National Institute of Standards and Technology (NIST) in USA. This software product can simulate the environment induced by a fire realistically. No turbulence models are required as high velocity flows were filtered out (acoustics filtering technique). Larger-scale turbulent flow structure induced by buoyancy was simulated directly by the set of low Mach number flow equations. The small-scale eddy motion was simulated by large eddy simulations (LES) with a sub-grid scale model [e.g. 8,9]. Additional subroutines on combustion chemistry, thermal radiation, and fire suppression are also included.

There are always challenges on how good a fire model can predict. However, very few experimental verifications [e.g. 1,4,5,8] were reported in the literature on validating fire field models. Most of the measured data are only for studying related topics such as fire-induced doorway flow, not for validating field models [e.g. 10,11]. New experimental studies [e.g. 12] other than those carried out earlier might be useful in confirming the performance of fire field models.

A full-scale burning facility known as the PolyU/HEU Assembly Calorimeter [13] was established jointly by Harbin Engineering University (HEU) and The Hong Kong Polytechnic University (PolyU) in Harbin, Heilongjiang, China. It is located in a small town Lanxi, about 150 km away from Harbin. Heat release rate of burning combustibles up to 5 MW can be measured by the oxygen consumption method. An exhaust hood with a fan-duct system was constructed. A 'duct-section' with proper alignment of velocity sensors, pressure sensors, laser, gas sampling tubes and thermocouples were installed.

A series of full-scale burning tests were carried out on studying fire environment and performance of fire suppression system to assess different empirical equations for estimating the minimum heat release rates to get flashover in a compartment fire [12]. Some measured results are now selected to compare with the results predicted by FDS version 3.01.

2. BRIEF REVIEW OF KEY EQUATIONS IN FDS

Air flow induced by a fire would be compressible with the hot smoke taken as thermally expandable gas [6-9] in the model Fire Dynamics Simulator (FDS) version 3.01. A set of governing equations suitable for simulating fluid flow induced by buoyancy with low Mach number was proposed. The Boussinesq approximation is no more necessary and constraints on inviscid fluid are removed. Larger variations of both density and temperature are allowed. The governing equations are:

Conservation of mass

$$\frac{\partial \rho}{\partial t} + \nabla \cdot \rho \mathbf{u} = 0 \qquad (1)$$

where $\mathbf{u}$ is the gas velocity vector and ρ is the gas density.

Conservation of species

$$\frac{\partial}{\partial t}(\rho Y_s) + \nabla \cdot \rho Y_s \mathbf{u} = \nabla \cdot \rho D_s \nabla Y_s + \dot{m}_s''' \qquad (2)$$

where Y_s, $\dot{m}_s'''$ and D_s are the mass fraction, the production rate per unit volume and the diffusion coefficient into the mixture of the s^{th} species.

Conservation of momentum

$$\rho\left(\frac{\partial \mathbf{u}}{\partial t} + \frac{1}{2}\nabla|\mathbf{u}|^2 - \mathbf{u} \times \boldsymbol{\omega}\right) + \nabla p - \rho \mathbf{g} = \nabla \cdot \boldsymbol{\tau} \qquad (3)$$

where $\boldsymbol{\omega}$ is the vorticity, p is the pressure, $\mathbf{g}$ is the gravity vector and $\boldsymbol{\tau}$ is the stress tensor.

Conservation of energy

$$\rho c_p\left(\frac{\partial T}{\partial t} + \mathbf{u} \cdot \nabla T\right) - \frac{dp_0}{dt} = \dot{q} + \nabla \cdot (k \nabla T) \qquad (4)$$

where T is the temperature, p_0 is the average pressure, $\dot{q}$ is the prescribed volumetric heat source, k is the thermal conductivity and c_p is constant pressure specific heat.

Equation of state

$$p_0(t) = \rho R T \qquad (5)$$

where R is the gas constant.

Note that in the energy equation and the equation of state, the spatially and temporally varying pressure has been replaced by an average pressure p_0 which depends only on time. An approximation to the ideal gas law is made by decomposing the pressure p into a "background" component p_0, a hydrostatic component $\rho_\infty gz$, and a flow-induced perturbation $\tilde{p}$.

$$p = p_0 - \rho_\infty gz + \tilde{p} \qquad (6)$$

This assumption is reasonable for flows with low Mach number because the temperature is inversely proportional to density. Replacing p in the energy equation and the equation of state by p_0 to filter out sound waves travelling at speeds much faster than typical flow speeds expected in fire applications would give fairly accurate predictions. The momentum equations are rearranged by assuming that vorticity generation due to buoyancy prevails over the baroclinic effect.

In large eddy simulation (LES), a flow variable $\phi(\mathbf{x}, t)$ would be decomposed by filtering into a resolved component (large-scale component) $\bar{\phi}(\mathbf{x}, t)$ and a subgrid-scale component $\phi'(\mathbf{x}, t)$ as:

$$\phi(\mathbf{x}, t) = \bar{\phi}(\mathbf{x}, t) + \phi'(\mathbf{x}, t) \qquad (7)$$

The resolved-scale component $\bar{\phi}(\mathbf{x}, t)$ is obtained by the following integral with a filter function $G(\mathbf{x} - \mathbf{x}', \Delta)$ as the filter kernel.

$$\bar{\phi}(\mathbf{x}, t) = \int_\Omega G(\mathbf{x} - \mathbf{x}', \Delta)\phi(\mathbf{x}', t)d\mathbf{x}' \qquad (8)$$

where Ω is the domain of interest, and Δ is the filter width given in terms of the volume of a computational cell V by:

$$\Delta = V^{1/3} = (\Delta x \Delta y \Delta z)^{1/3} \qquad (8a)$$

The grid widths Δx, Δy and Δz are along the directions of x, y and z.

The filter function is:

$$G(\mathbf{x}-\mathbf{x}',\Delta)=\begin{cases}1/V & \text{for } \mathbf{x}'\in V\\ 0 & \text{otherwise}\end{cases} \quad (9)$$

The mixture fraction model [6-9] is used to describe the burning process of fire. The model is based on the assumption that the combustion is mixing-controlled. All species of interest are described by a mixture fraction $f(\mathbf{x},t)$, which is a conserved quantity representing the fraction of species at a given point originated from the fuel. The relations between the mass fraction of each species and the mixture fraction are known as "state relations". The state relation for the oxygen mass fraction would provide the necessary information to calculate the local oxygen mass consumption rate. The local heat release rate $\dot{q}'''$ is computed from the local oxygen consumption rate by assuming that $\dot{q}'''$ is directly proportional to the oxygen consumption rate and independent of the fuel involved.

Taking the global one-step irreversible chemical reaction as an example:

$$v_F\,\text{Fuel} + v_O O_2 \rightarrow v_P\,\text{Products}$$

In the above reaction, v_F, v_O and v_P are stoichiometric coefficients for fuel, oxygen and products respectively. The mixture fraction *f* is defined as:

$$f=\frac{sY_F-(Y_O-Y_O^{\infty})}{sY_F^{I}+Y_O^{\infty}} \quad (10)$$

where Y_F, Y_O, Y_O^{∞}, Y_F^{I} are mass fractions of fuel, oxygen, oxygen in the ambient air and fuel at the source respectively. s is the stoichiometric ratio given in terms of the molecular weight of fuel and oxygen W_F, W_O by:

$$s=\frac{v_O W_O}{v_F W_F}$$

With the infinite fast-chemistry assumption, f satisfies the conservation law:

$$\frac{\partial \rho f}{\partial t}+\nabla\cdot(\rho\mathbf{u}f)=\nabla\cdot(\rho D\nabla f) \quad (11)$$

Consider the transport equations for oxygen with concentration Y_O:

$$\rho\frac{DY_O}{Dt}=\nabla\cdot\rho D\nabla Y_O+\dot{m}_O''' \quad (12)$$

Multiplying equation (11) by $\frac{dY_O}{df}$ and assuming the diffusion coefficient D is constant with respect to the species, combining with equation (12) gives the mass loss rate of oxygen $\dot{m}_O'''$:

$$-\dot{m}_O'''=\nabla\cdot\left(\rho D\frac{dY_O}{df}\nabla f\right)-\frac{dY_O}{df}\nabla\cdot\rho D\nabla f \quad (13)$$

The oxygen consumption rate can be determined from equations (12) and (13), and multiplying by the heat release rate per unit mass of oxygen consumed ΔH_O would yield the local heat release rate $\dot{q}'''$:

$$\dot{q}'''=\Delta H_O\dot{m}_O''' \quad (14)$$

3. NUMERICAL EXPERIMENTS

Numerical experiments were carried out on some full-scale burning tests at the PolyU/HEU Assembly Calorimeter [12,13]. A room of length 3.6 m, width 2.4 m and height 2.4 m similar to the standard room calorimeter for the room-corner fire test as in Fig. 1a was considered. There is a door of height 2.0 m and width 0.8 m.

A liquid pool fire of 1 m diameter was placed at the centre of the room. Seven thermocouples were used to measure the indoor temperature with three (T_a, T_b and T_c) placed at the ceiling. Another four (T_d, T_e, T_f and T_g) arranged as a thermocouple tree were placed at 0.7 m from the door and 0.7 m from the left wall.

The computing domain was extended 2.2 m out of the chamber. Free boundary conditions are specified properly on four surfaces. In this way, the neutral plane height in the doorway can be predicted. The pool fire was approximated by a 0.8 m square, having similar area as the circular container in the experiments, to match with the grid system. Three-dimensional cartessian co-ordinate system was used with x-direction along the length, y-direction across the width and z-direction moving up the height as in Fig. 1b. The computing domains are 75, 30 and 30, distributed uniformly along the x-, y-, and z-dimensions, giving 67,500 cells.

Two scenarios are considered:

- S1: Initial indoor temperature of 15 ^{o}C.
- S2: Initial indoor temperature of 50 ^{o}C for simulating experiments for the chamber not yet cooled down.

The heat release rate curve measured in this set of experiment is shown in Fig. 2. The peak heat release rate was about 2.5 MW and burning duration of about 3 minutes. This curve is taken as the input function to the FDS model. An input file on S1 is shown in Appendix A.

Simulations were carried out in a personal computer with a processor of 1.9 GHz, 512 MB RAM and harddisk 80 GB. The computing time required was up to 24 hrs. Transient predicted results can be visualized by a post-processor Smokeview. Results were analyzed by a graphics processor specially designed for compiling CFD/NHT predicted files.

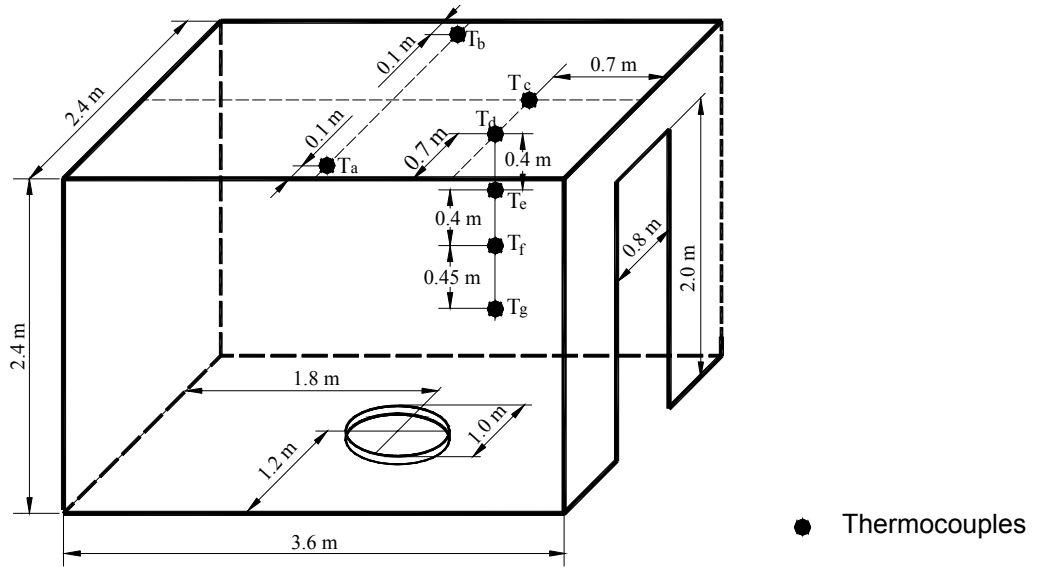

(a) Geometry

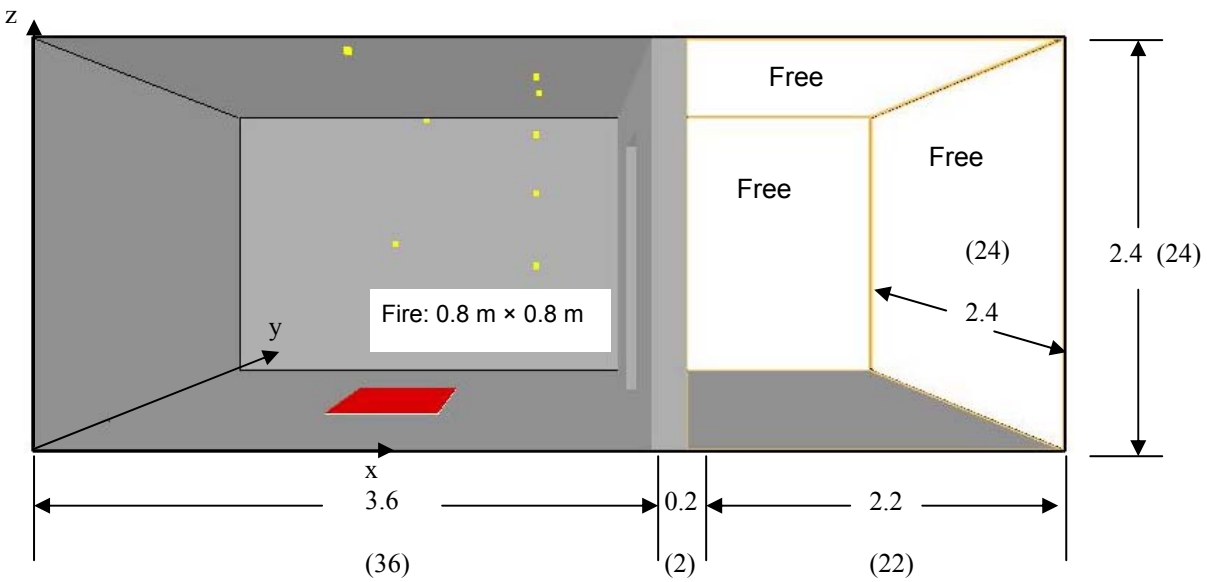

(b) Computing domains

Fig. 1: Full-scale burning facility

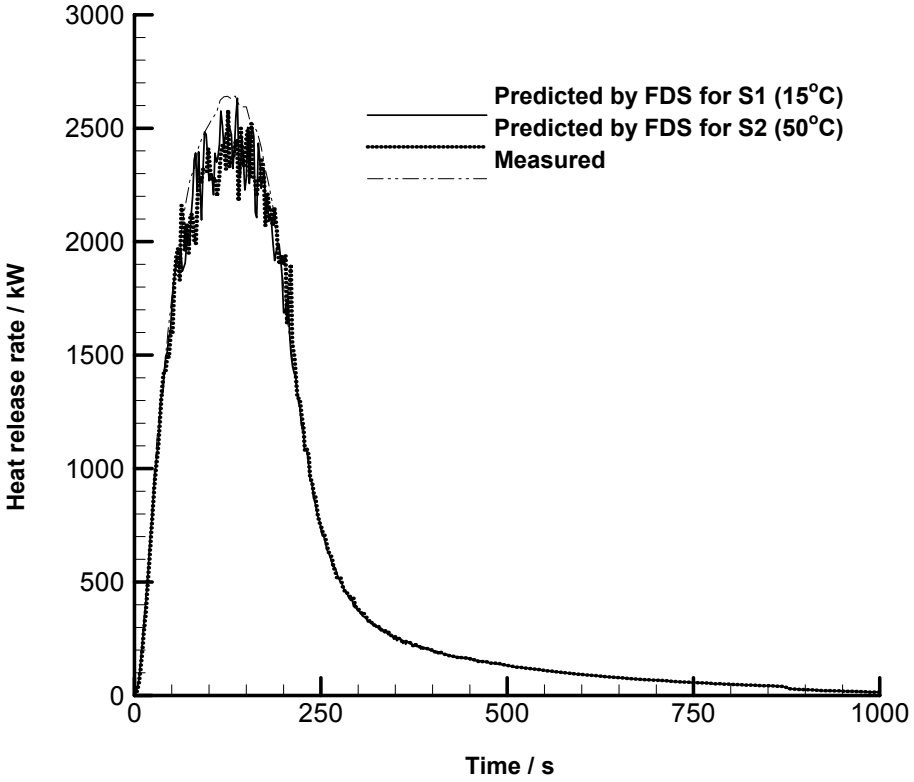

Fig. 2: Heat release rate

4. RESULTS

The heat release rate curves for S1 and S2 were calculated by FDS using thermal element method. Results are shown also in Fig. 2 and the two predicted curves are very similar to the measured one.

Results on the fire environment denoted by the velocity vectors and temperature contours induced by the pool fires across the central y-plane at 4 s, 10 s, 100 s, 140 s and 260 s are shown in Fig. 3 for S1 and Fig. 4 for S2. Transient development of the flow and temperature fields matched with the heat release rate curve. Heat release rate started to increase upon igniting the liquid fuel, and then decreased when the fuel was used up.

In fact, two more sets of numerical experiments on each scenario were carried out with similar heat release rate curves on comparing with the measured results for two other sets of experiments with the same pool fire and ventilation factor. Results are similar to the above.

5. DISCUSSIONS

For S1, a plume was simulated first as shown by the velocity vectors at 4 s in Fig. 3a. Basically, there are two air circulations across this vertical plane. One air circulation loop was found between the fire and the wall, and the other one between the door and the fire. Later, air circulation between the fire and the wall disappeared, leaving only one as in Figs. 3c and d. Air would flow in, heated up, rise and then move out of the room. But when the fuel was about to be used up after 140 s, the flow structures became quite complicated as in Figs. 3d and e.

Similar pattern to S1 was predicted inside the chamber for S2. However, the air flow pattern at the extended computing domain was quite complicated. There are entrainment effect at the ends for this scenario. Further measurement should be carried out to decide which set of prediction is correct.

Transient temperatures measured at the seven thermocouples are shown in Fig. 5 for the ceiling; and Figs. 6 and 7 on the thermocouple tree for S1 and S2 respectively. Results predicted by FDS are also shown in those figures. The general trends of those measured and predicted temperature-time curves are similar. Deviations of over 100 ^{o}C were found at some stages of the fire.

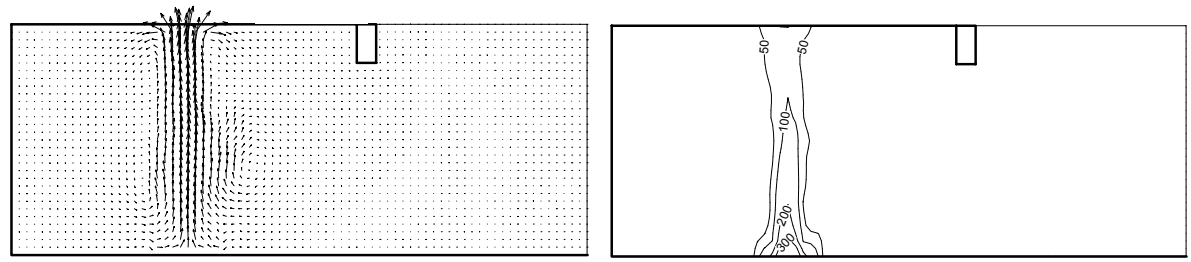

(a) 4s

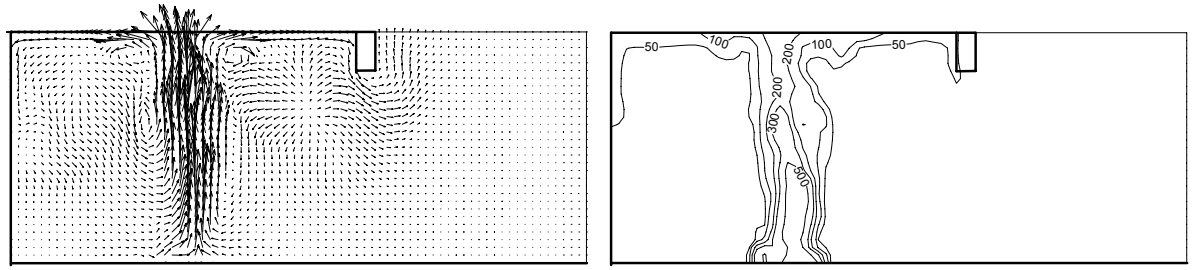

(b) 10s

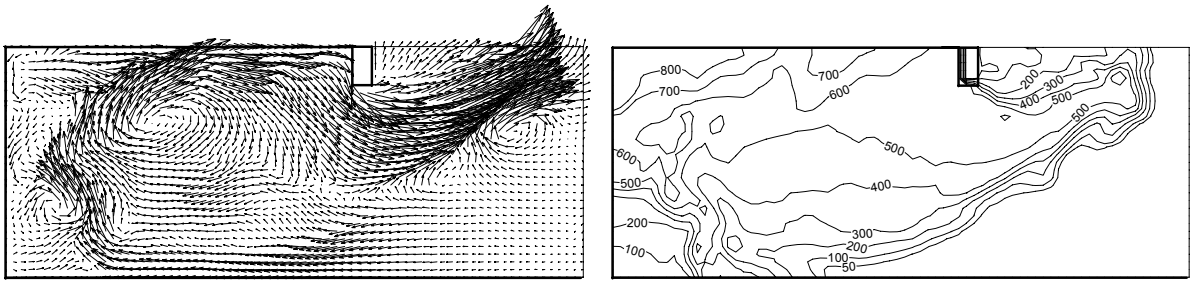

(c) 100s

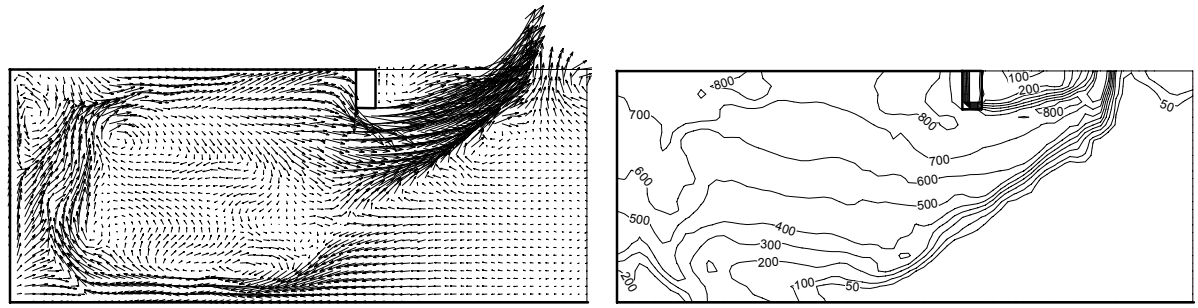

(d) 140s

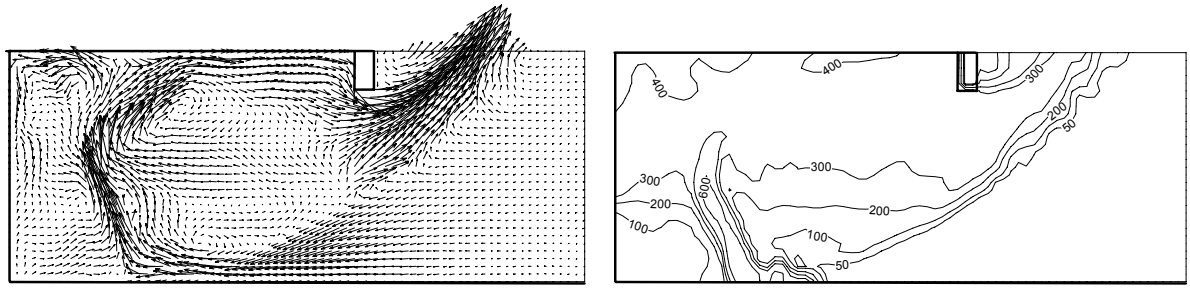

(e) 260s

⟶ 4.0 ms^{-1}

Fig. 3: Predicted fire environment for S1

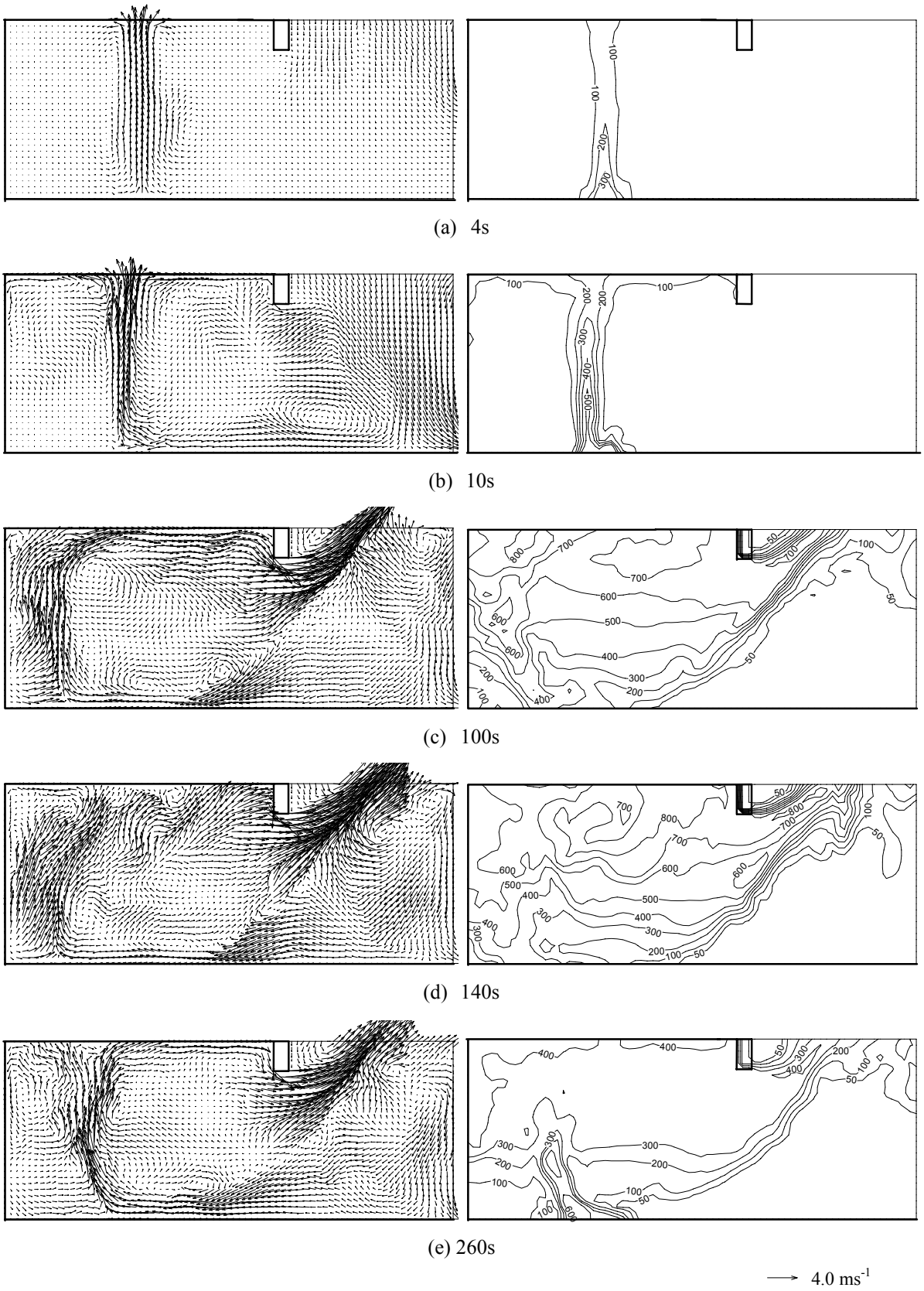

Fig. 4: Predicted fire environment for S2

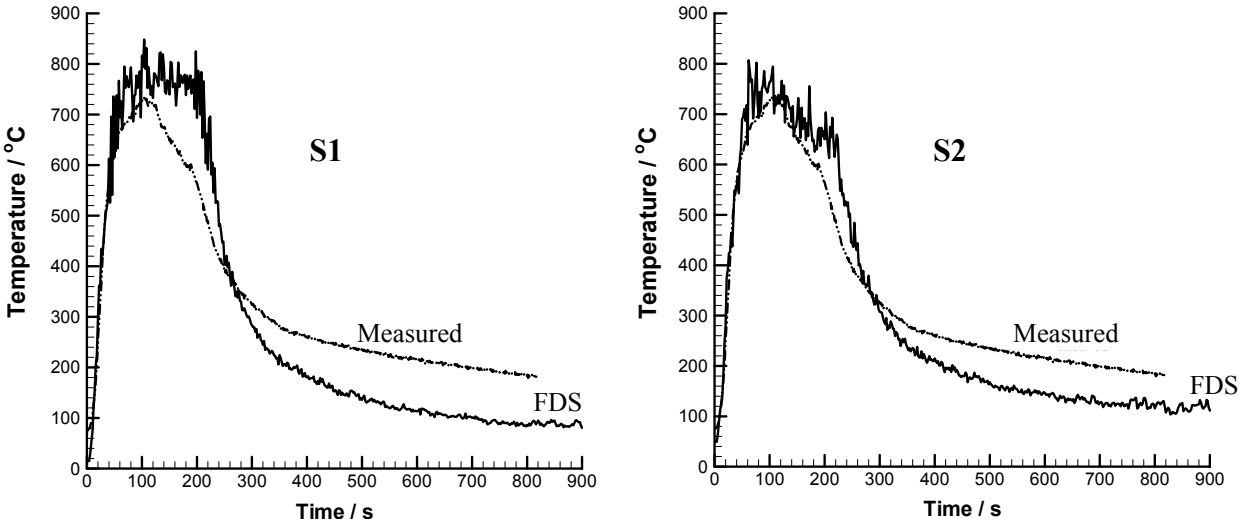

(a) At point T_a

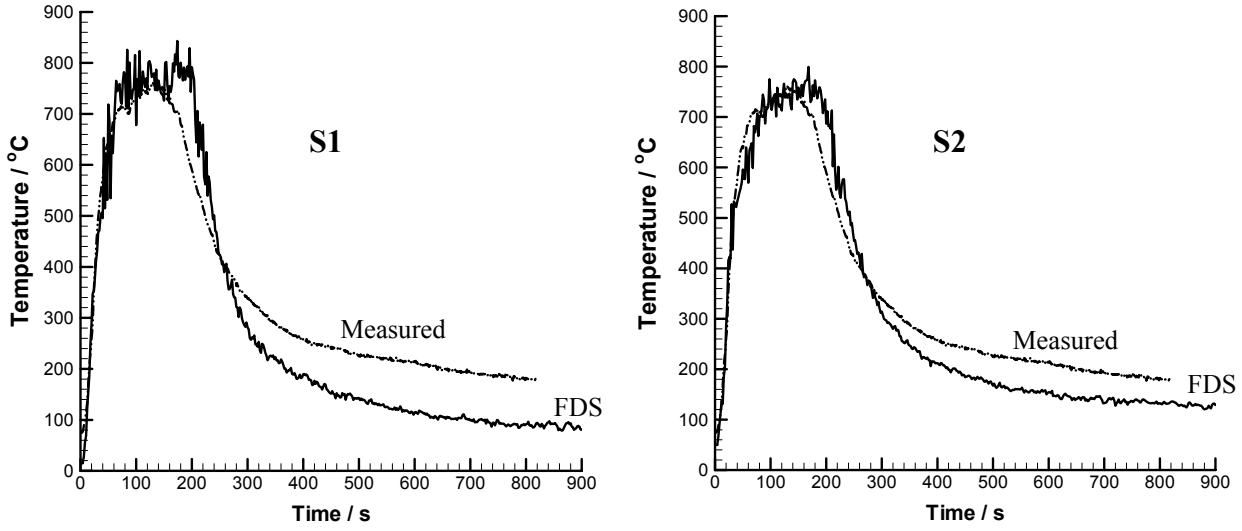

(b) At point T_b

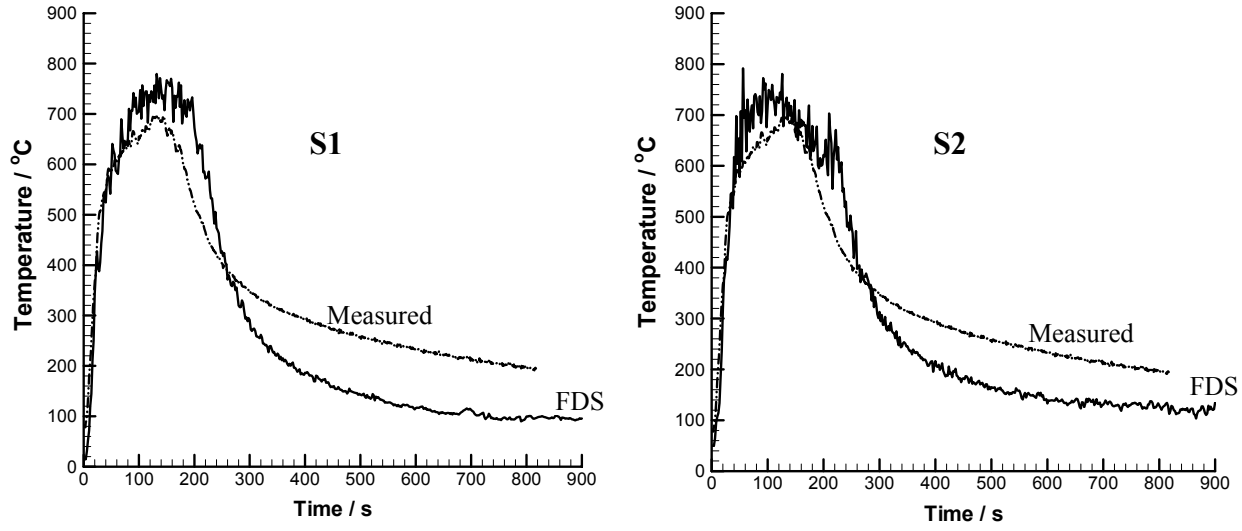

(c) At point T_c

Fig. 5: Thermocouples at ceiling

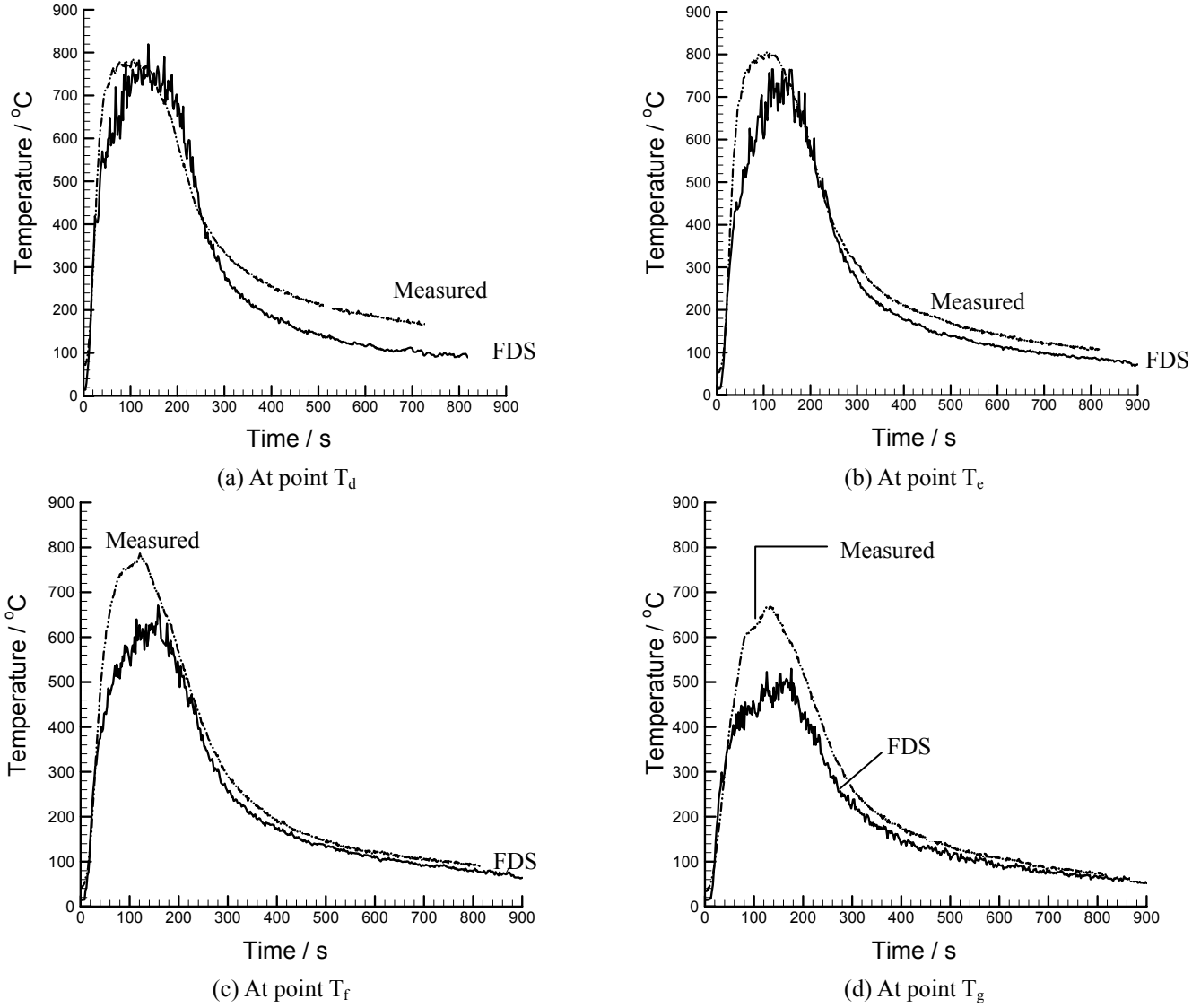

Fig. 6: Results at thermocouple tree for S1

There are also differences in the predicted temperature contours for S1 and S2 in the extended region. Predicted temperatures were different from the measured ones at lower levels. The differences might be over 150 °C between S1 and S2.

The predicted temperatures for S1 and S2 are plotted against the measured data in Fig. 8. This gives a practical presentation on how good FDS can predict.

It is observed that the model FDS version 3.01 can give fairly good predictions on the fire-induced air flow and temperature fields in this study on room fires with liquid pools. Although deviations from measured data at ceiling levels and lower levels are not quite the same in different stages of the room fires, the general trend of the time history of temperature is still acceptable.

6. CONCLUSIONS

Studies in this paper on comparing with full-scale burning data in room fires [12] indicated that compartment fires can be simulated fairly accurately by FDS. Note that a two-layer zone model [e.g. 1] might not be applicable to simulate the fire environment for flashover fires in a bigger building. It is not good for studying flashover when there is no hot smoke layer. On the other hand, a zone model cannot give velocity vectors and temperature distributions. There are many empirical parameters to be tuned up for CFD/NHT models based on RANS type of equations. It appears that FDS can give quite good predictions, and perhaps it is suitable for use as a practical tool in fire safety designs.

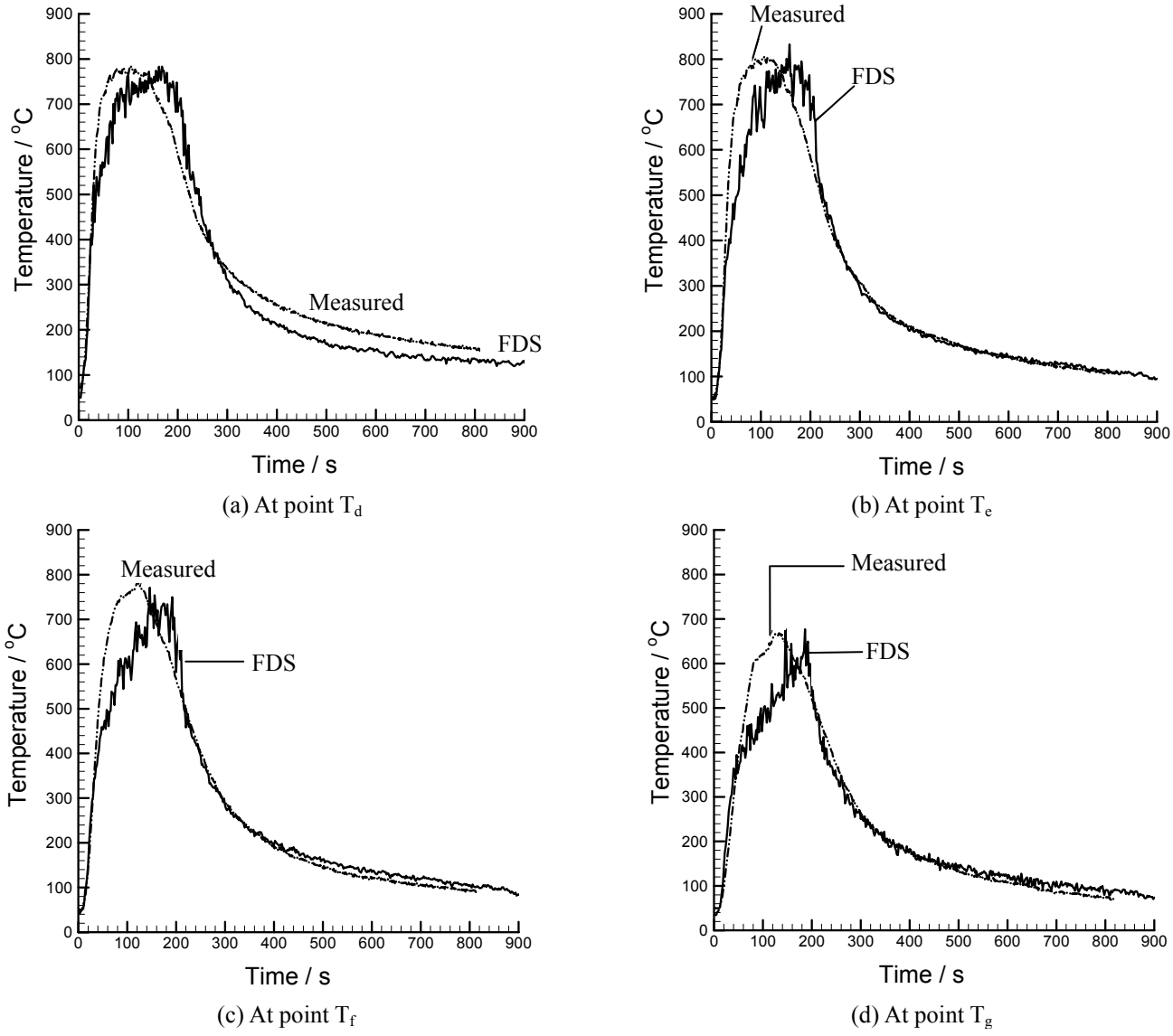

Fig. 7: Results at thermocouple tree for S2

Literature [8,9] indicated that FDS [6,7] is capable of predicting buoyancy-induced turbulent flow structure. The software should be applicable for designing smoke management systems [e.g. 14]. This part will be discussed separately in later publications on smoke management systems, deriving empirical correlation on doorway flow rates and on predicting flashover. The earlier version 1.0 of FDS was tested before [15] with results not much different from those predicted by using turbulent models based on RANS. By that time, FDS version 1.0 was not yet popular as the computing requirement was quite demanding, making it not too suitable for running in a personal computer. With the rapid development of computer hardware, this is no more a concern. Obviously, there are always rooms for improvement such as including intermediate chemistry [16] even for fuels with simple chemical structures.

ACKNOWLEDGEMENT

This paper is partly supported by the PolyU president under research account A-078 as an Area of Strength in Fire Safety Engineering, and partly by the departmental earnings account, Department of Building Services Engineering contributed from the self-financed MSc degree programme in Fire and Safety Engineering.

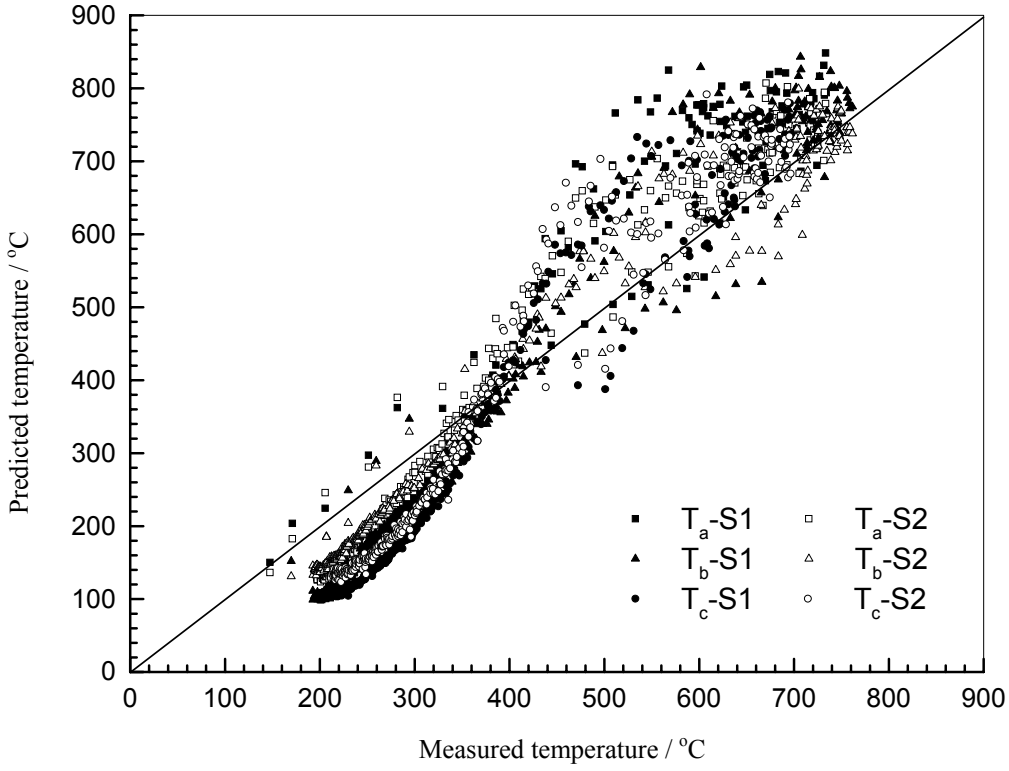

(a) Ceiling: T_a to T_c

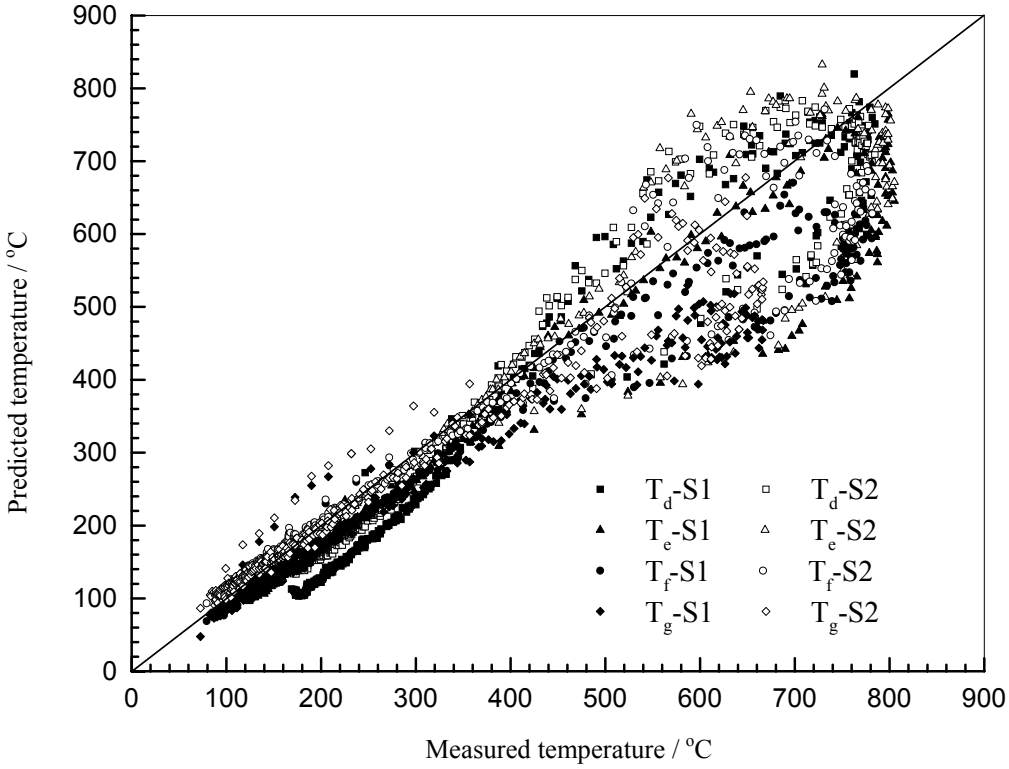

(b) Thermocouple tree: T_d to T_g

Fig. 8: Comparison of predicted temperatures with measurement

NOMENCLATURE

c_p specific heat capacity at constant pressure
D_s diffusion coefficient into the mixture of the s^{th} species
f mixture fraction
g acceleration due to gravity
ΔH_O heat release rate per unit mass of oxygen consumed
k thermal conductivity
$\dot{m}_O'''$ mass loss rate of oxygen
$\dot{m}_s'''$ production rate per unit volume of the s^{th} species
p pressure
p_0 average pressure
$\tilde{p}$ pressure perturbation
$\dot{q}$ volumetric heat source
$\dot{q}'''$ heat release rate per unit volume
R gas constant
t time
T temperature
u velocity vector
v_F stoichiometric coefficients for fuel
v_O stoichiometric coefficients for oxygen
v_P stoichiometric coefficients for products
$\mathbf{x}, \mathbf{x}'$ position vectors
Y_F mass fraction of fuel
Y_O mass fraction of oxygen
Y_s mass fraction of the s^{th} species
Y_F^I mass fraction of fuel in the fuel stream
Y_O^∞ mass fraction of oxygen in the ambient

Greek symbols

ρ density
τ stress tensor
ω vorticity

REFERENCES

1. G. Cox, Combustion fundamentals of fires, Academic Press, London (1995).
2. W.K. Chow and W.Q. Tao, "Application of fire field modeling in fire safety engineering: Computational Fluid Dynamics (CFD) or Numerical Heat Transfer (NHT)?", CPD lecture, 29 March (2003).
3. Practice note for authorized persons and registered structural engineers: Guide to fire engineering approach, Guide BD GP/BREG/P/36, Buildings Department, Hong Kong Special Administrative Region, March (1998).
4. W.K. Chow and W.M. Leung, "Solid-wall boundary effect on a building fire field model", Combustion Science and Technology, Vol. 71, No. 1-3, pp. 77-93 (1990).
5. S. Nam and R.G. Jr Bill, "Numerical simulation of thermal plumes", Fire Safety Journal, Vol. 21, No. 3, pp. 231-256 (1993).
6. K.B. McGrattan H.R. Baum, R.G. Rehm, A. Hammins, G.P. Forney, J.E. Floyd, S. Hostikka and K. Prasad, Fire Dynamics Simulator (Version 3) - Technical reference guide, NISTIR 6783, National Institute of Standards and Technology, US Department of Commerce, November (2001).
7. K.B. McGrattan, G.P. Forney, J.E. Floyd, S. Hostikka and K. Prasad, Fire Dynamics Simulator (Version 3) – User's guide, NISTIR 6784, National Institute of Standards and Technology, US Department of Commerce, November (2002).
8. K.B. McGrattan, H.R. Baum and R.G. Rehm, "Large eddy simulations of smoke movement", Fire Safety Journal, Vol. 30, pp. 161-178 (1998).
9. H.R. Baum, "Large eddy simulations of fires – from concepts to computations", Fire Protection Engineering, No. 6, pp. 36-38, 40, 42 (2000).
10. K.D. Steckler, J.Q, Quintiere and W.D. Rinkinen, "Flow induced by a fire in a compartment", 19th International Symposium on Combustion, The Combustion Institute, Pittsburgh, pp. 913-920 (1982).
11. K.D. Steckler, H.R. Baum and J.Q, Quintiere, "Fire induced flows through room openings – flow coefficients", 20th International Symposium on Combustion, The Combustion Institute, Pittsburgh, pp. 1591-1600 (1984).
12. W.K. Chow, Y. Gao, H. Dong, G. Zou, Z. Luo and L. Meng, "Experimental studies on minimum heat release rates for flashover with oxygen consumption calorimetry", Architectural Science Review, Vol. 46, No. 3, pp. 291-296 (2003).
13. W.K. Chow, "Support on carrying out full-scale burning tests for karaokes", International Journal on Engineering Performance-Based Fire Codes, Vol. 3, No. 3, pp. 104-112 (2001).
14. J.A. Milke, "Using models to support smoke management system design", Fire Protection Engineering, No. 7, pp. 17-18, 21-22 (2000).
15. R. Yin and W.K. Chow, "Building fire simulation with a field model based on large eddy simulation", Architectural Science Review, Vol. 45, No. 2, pp. 145-153 (2002).
16. W.R. Zeng, S.F. Li and W.K. Chow, "Review on chemical reactions of burning Poly(methyl methacrylate) PMMA", Journal of Fire Sciences, Vol. 20, No. 5, pp. 401-433 (2002).

APPENDIX A: INPUT FILE

```
&HEAD CHID='Iso', TITLE='Door=0.80*2.00m, grid=0.08*0.08*0.08m, Burner=2642kW' /
&GRID IBAR=75, JBAR=30, KBAR=30 /
&PDIM XBAR=6.00, YBAR=2.40, ZBAR=2.40 /

&TIME TWFIN=1200. /

&MISC REACTION='KEROSENE',
    SURF_DEFAULT='CONCRETE',
    DATABASE='C:\nist\Iso\database.data' /

&MISC TMPA=15. / ambient temperature
&MISC TMPO=15. / outside temperature

&MISC RADIATION=.TRUE. /

&MISC DTCORE=2.0 /

&SURF ID='burner',HRRPUA=4128.125, RGB=1,0,0, RAMP_Q='burner RAMP'/ HRR=2642kW
&VENT XB= 1.40,2.20,  0.80,1.60,  0.00,0.00, SURF_ID='burner' /

&RAMP ID='burner RAMP', T= 0    , F= 0.0000 /
&RAMP ID='burner RAMP', T= 5    , F= 0.0204 /
&RAMP ID='burner RAMP', T= 10   , F= 0.0871 /
&RAMP ID='burner RAMP', T= 15   , F= 0.1673 /
&RAMP ID='burner RAMP', T= 20   , F= 0.2566 /
&RAMP ID='burner RAMP', T= 25   , F= 0.3441 /
&RAMP ID='burner RAMP', T= 30   , F= 0.4251 /
&RAMP ID='burner RAMP', T= 35   , F= 0.4962 /
&RAMP ID='burner RAMP', T= 40   , F= 0.5568 /
&RAMP ID='burner RAMP', T= 45   , F= 0.6090 /
&RAMP ID='burner RAMP', T= 50   , F= 0.6631 /
&RAMP ID='burner RAMP', T= 55   , F= 0.7074 /
&RAMP ID='burner RAMP', T= 60   , F= 0.7502 /
&RAMP ID='burner RAMP', T= 65   , F= 0.7937 /
&RAMP ID='burner RAMP', T= 70   , F= 0.8293 /
&RAMP ID='burner RAMP', T= 75   , F= 0.8637 /
&RAMP ID='burner RAMP', T= 80   , F= 0.8812 /
&RAMP ID='burner RAMP', T= 85   , F= 0.9118 /
&RAMP ID='burner RAMP', T= 90   , F= 0.9281 /
&RAMP ID='burner RAMP', T= 95   , F= 0.9444 /
&RAMP ID='burner RAMP', T= 100  , F= 0.9527 /
&RAMP ID='burner RAMP', T= 105  , F= 0.9633 /
&RAMP ID='burner RAMP', T= 110  , F= 0.9724 /
&RAMP ID='burner RAMP', T= 115  , F= 0.9932 /
&RAMP ID='burner RAMP', T= 120  , F= 0.9989 /
&RAMP ID='burner RAMP', T= 125  , F= 0.9996 /
&RAMP ID='burner RAMP', T= 130  , F= 0.9955 /
&RAMP ID='burner RAMP', T= 135  , F= 1.     /
&RAMP ID='burner RAMP', T= 140  , F= 0.9860 /
&RAMP ID='burner RAMP', T= 145  , F= 0.9818 /
&RAMP ID='burner RAMP', T= 150  , F= 0.9818 /
&RAMP ID='burner RAMP', T= 155  , F= 0.9580 /
&RAMP ID='burner RAMP', T= 160  , F= 0.9519 /
&RAMP ID='burner RAMP', T= 165  , F= 0.9387 /
&RAMP ID='burner RAMP', T= 170  , F= 0.9148 /
&RAMP ID='burner RAMP', T= 175  , F= 0.8815 /
&RAMP ID='burner RAMP', T= 180  , F= 0.8531 /
```

```
&RAMP ID='burner RAMP', T= 185  , F= 0.8213 /
&RAMP ID='burner RAMP', T= 190  , F= 0.7729 /
&RAMP ID='burner RAMP', T= 195  , F= 0.7358 /
&RAMP ID='burner RAMP', T= 200  , F= 0.6836 /
&RAMP ID='burner RAMP', T= 205  , F= 0.6276 /
&RAMP ID='burner RAMP', T= 210  , F= 0.5791 /
&RAMP ID='burner RAMP', T= 215  , F= 0.5299 /
&RAMP ID='burner RAMP', T= 220  , F= 0.4868 /
&RAMP ID='burner RAMP', T= 225  , F= 0.4417 /
&RAMP ID='burner RAMP', T= 230  , F= 0.4065 /
&RAMP ID='burner RAMP', T= 235  , F= 0.3660 /
&RAMP ID='burner RAMP', T= 240  , F= 0.3354 /
&RAMP ID='burner RAMP', T= 245  , F= 0.3047 /
&RAMP ID='burner RAMP', T= 250  , F= 0.2793 /
&RAMP ID='burner RAMP', T= 255  , F= 0.2581 /
&RAMP ID='burner RAMP', T= 260  , F= 0.2369 /
&RAMP ID='burner RAMP', T= 265  , F= 0.2199 /
&RAMP ID='burner RAMP', T= 270  , F= 0.2055 /
&RAMP ID='burner RAMP', T= 275  , F= 0.1915 /
&RAMP ID='burner RAMP', T= 280  , F= 0.1790 /
&RAMP ID='burner RAMP', T= 285  , F= 0.1696 /
&RAMP ID='burner RAMP', T= 290  , F= 0.1597 /
&RAMP ID='burner RAMP', T= 295  , F= 0.1499 /
&RAMP ID='burner RAMP', T= 300  , F= 0.1412 /
&RAMP ID='burner RAMP', T= 305  , F= 0.1347 /
&RAMP ID='burner RAMP', T= 310  , F= 0.1291 /
&RAMP ID='burner RAMP', T= 315  , F= 0.1234 /
&RAMP ID='burner RAMP', T= 320  , F= 0.1181 /
&RAMP ID='burner RAMP', T= 325  , F= 0.1139 /
&RAMP ID='burner RAMP', T= 330  , F= 0.1098 /
&RAMP ID='burner RAMP', T= 335  , F= 0.1060 /
&RAMP ID='burner RAMP', T= 340  , F= 0.1026 /
&RAMP ID='burner RAMP', T= 345  , F= 0.0988 /
&RAMP ID='burner RAMP', T= 350  , F= 0.0961 /
&RAMP ID='burner RAMP', T= 355  , F= 0.0939 /
&RAMP ID='burner RAMP', T= 360  , F= 0.0908 /
&RAMP ID='burner RAMP', T= 365  , F= 0.0878 /
&RAMP ID='burner RAMP', T= 370  , F= 0.0855 /
&RAMP ID='burner RAMP', T= 375  , F= 0.0840 /
&RAMP ID='burner RAMP', T= 380  , F= 0.0810 /
&RAMP ID='burner RAMP', T= 385  , F= 0.0795 /
&RAMP ID='burner RAMP', T= 390  , F= 0.0780 /
&RAMP ID='burner RAMP', T= 395  , F= 0.0753 /
&RAMP ID='burner RAMP', T= 400  , F= 0.0742 /
&RAMP ID='burner RAMP', T= 405  , F= 0.0719 /
&RAMP ID='burner RAMP', T= 410  , F= 0.0704 /
&RAMP ID='burner RAMP', T= 415  , F= 0.0685 /
&RAMP ID='burner RAMP', T= 420  , F= 0.0670 /
&RAMP ID='burner RAMP', T= 425  , F= 0.0655 /
&RAMP ID='burner RAMP', T= 430  , F= 0.0640 /
&RAMP ID='burner RAMP', T= 435  , F= 0.0632 /
&RAMP ID='burner RAMP', T= 440  , F= 0.0617 /
&RAMP ID='burner RAMP', T= 445  , F= 0.0609 /
&RAMP ID='burner RAMP', T= 450  , F= 0.0602 /
&RAMP ID='burner RAMP', T= 455  , F= 0.0583 /
&RAMP ID='burner RAMP', T= 460  , F= 0.0572 /
&RAMP ID='burner RAMP', T= 465  , F= 0.0564 /
&RAMP ID='burner RAMP', T= 470  , F= 0.0556 /
&RAMP ID='burner RAMP', T= 475  , F= 0.0541 /
```

```
&RAMP ID='burner RAMP', T= 480  , F= 0.0534 /
&RAMP ID='burner RAMP', T= 485  , F= 0.0526 /
&RAMP ID='burner RAMP', T= 490  , F= 0.0515 /
&RAMP ID='burner RAMP', T= 495  , F= 0.0503 /
&RAMP ID='burner RAMP', T= 500  , F= 0.0492 /
&RAMP ID='burner RAMP', T= 505  , F= 0.0481 /
&RAMP ID='burner RAMP', T= 510  , F= 0.0469 /
&RAMP ID='burner RAMP', T= 515  , F= 0.0466 /
&RAMP ID='burner RAMP', T= 520  , F= 0.0458 /
&RAMP ID='burner RAMP', T= 525  , F= 0.0450 /
&RAMP ID='burner RAMP', T= 530  , F= 0.0443 /
&RAMP ID='burner RAMP', T= 535  , F= 0.0435 /
&RAMP ID='burner RAMP', T= 540  , F= 0.0428 /
&RAMP ID='burner RAMP', T= 545  , F= 0.0420 /
&RAMP ID='burner RAMP', T= 550  , F= 0.0413 /
&RAMP ID='burner RAMP', T= 555  , F= 0.0405 /
&RAMP ID='burner RAMP', T= 560  , F= 0.0401 /
&RAMP ID='burner RAMP', T= 565  , F= 0.0390 /
&RAMP ID='burner RAMP', T= 570  , F= 0.0386 /
&RAMP ID='burner RAMP', T= 575  , F= 0.0379 /
&RAMP ID='burner RAMP', T= 580  , F= 0.0371 /
&RAMP ID='burner RAMP', T= 585  , F= 0.0367 /
&RAMP ID='burner RAMP', T= 590  , F= 0.0356 /
&RAMP ID='burner RAMP', T= 595  , F= 0.0352 /
&RAMP ID='burner RAMP', T= 600  , F= 0.0348 /
&RAMP ID='burner RAMP', T= 605  , F= 0.0341 /
&RAMP ID='burner RAMP', T= 610  , F= 0.0337 /
&RAMP ID='burner RAMP', T= 615  , F= 0.0333 /
&RAMP ID='burner RAMP', T= 620  , F= 0.0326 /
&RAMP ID='burner RAMP', T= 625  , F= 0.0322 /
&RAMP ID='burner RAMP', T= 630  , F= 0.0314 /
&RAMP ID='burner RAMP', T= 635  , F= 0.0310 /
&RAMP ID='burner RAMP', T= 640  , F= 0.0303 /
&RAMP ID='burner RAMP', T= 645  , F= 0.0299 /
&RAMP ID='burner RAMP', T= 650  , F= 0.0295 /
&RAMP ID='burner RAMP', T= 655  , F= 0.0291 /
&RAMP ID='burner RAMP', T= 660  , F= 0.0284 /
&RAMP ID='burner RAMP', T= 665  , F= 0.0280 /
&RAMP ID='burner RAMP', T= 670  , F= 0.0276 /
&RAMP ID='burner RAMP', T= 675  , F= 0.0269 /
&RAMP ID='burner RAMP', T= 680  , F= 0.0269 /
&RAMP ID='burner RAMP', T= 685  , F= 0.0261 /
&RAMP ID='burner RAMP', T= 690  , F= 0.0261 /
&RAMP ID='burner RAMP', T= 695  , F= 0.0257 /
&RAMP ID='burner RAMP', T= 700  , F= 0.0254 /
&RAMP ID='burner RAMP', T= 705  , F= 0.0250 /
&RAMP ID='burner RAMP', T= 710  , F= 0.0246 /
&RAMP ID='burner RAMP', T= 715  , F= 0.0242 /
&RAMP ID='burner RAMP', T= 720  , F= 0.0235 /
&RAMP ID='burner RAMP', T= 725  , F= 0.0231 /
&RAMP ID='burner RAMP', T= 730  , F= 0.0227 /
&RAMP ID='burner RAMP', T= 735  , F= 0.0223 /
&RAMP ID='burner RAMP', T= 740  , F= 0.0223 /
&RAMP ID='burner RAMP', T= 745  , F= 0.0216 /
&RAMP ID='burner RAMP', T= 750  , F= 0.0216 /
&RAMP ID='burner RAMP', T= 755  , F= 0.0212 /
&RAMP ID='burner RAMP', T= 760  , F= 0.0208 /
&RAMP ID='burner RAMP', T= 765  , F= 0.0208 /
&RAMP ID='burner RAMP', T= 770  , F= 0.0204 /
```

```
&RAMP ID='burner RAMP', T= 775  , F= 0.0197 /
&RAMP ID='burner RAMP', T= 780  , F= 0.0193 /
&RAMP ID='burner RAMP', T= 785  , F= 0.0197 /
&RAMP ID='burner RAMP', T= 790  , F= 0.0189 /
&RAMP ID='burner RAMP', T= 795  , F= 0.0189 /
&RAMP ID='burner RAMP', T= 800  , F= 0.0185 /
&RAMP ID='burner RAMP', T= 805  , F= 0.0178 /
&RAMP ID='burner RAMP', T= 810  , F= 0.0182 /
&RAMP ID='burner RAMP', T= 815  , F= 0.0174 /
&RAMP ID='burner RAMP', T= 820  , F= 0.0174 /
&RAMP ID='burner RAMP', T= 825  , F= 0.0174 /
&RAMP ID='burner RAMP', T= 830  , F= 0.0170 /
&RAMP ID='burner RAMP', T= 835  , F= 0.0167 /
&RAMP ID='burner RAMP', T= 840  , F= 0.0163 /
&RAMP ID='burner RAMP', T= 845  , F= 0.0159 /
&RAMP ID='burner RAMP', T= 850  , F= 0.0163 /
&RAMP ID='burner RAMP', T= 855  , F= 0.0159 /
&RAMP ID='burner RAMP', T= 860  , F= 0.0155 /
&RAMP ID='burner RAMP', T= 865  , F= 0.0151 /
&RAMP ID='burner RAMP', T= 870  , F= 0.0151 /
&RAMP ID='burner RAMP', T= 875  , F= 0.0121 /
&RAMP ID='burner RAMP', T= 880  , F= 0.0106 /
&RAMP ID='burner RAMP', T= 885  , F= 0.0106 /
&RAMP ID='burner RAMP', T= 890  , F= 0.0102 /
&RAMP ID='burner RAMP', T= 895  , F= 0.0098 /
&RAMP ID='burner RAMP', T= 900  , F= 0.0095 /
&RAMP ID='burner RAMP', T= 905  , F= 0.0095 /
&RAMP ID='burner RAMP', T= 910  , F= 0.0091 /
&RAMP ID='burner RAMP', T= 915  , F= 0.0087 /
&RAMP ID='burner RAMP', T= 920  , F= 0.0083 /
&RAMP ID='burner RAMP', T= 925  , F= 0.0079 /
&RAMP ID='burner RAMP', T= 930  , F= 0.0079 /
&RAMP ID='burner RAMP', T= 935  , F= 0.0079 /
&RAMP ID='burner RAMP', T= 940  , F= 0.0076 /
&RAMP ID='burner RAMP', T= 945  , F= 0.0076 /
&RAMP ID='burner RAMP', T= 950  , F= 0.0072 /
&RAMP ID='burner RAMP', T= 955  , F= 0.0068 /
&RAMP ID='burner RAMP', T= 960  , F= 0.0068 /
&RAMP ID='burner RAMP', T= 965  , F= 0.0068 /
&RAMP ID='burner RAMP', T= 970  , F= 0.0064 /
&RAMP ID='burner RAMP', T= 975  , F= 0.0064 /
&RAMP ID='burner RAMP', T= 980  , F= 0.0061 /
&RAMP ID='burner RAMP', T= 985  , F= 0.0057 /
&RAMP ID='burner RAMP', T= 990  , F= 0.0057 /
&RAMP ID='burner RAMP', T= 995  , F= 0.0057 /
&RAMP ID='burner RAMP', T= 1000 , F= 0.0057 /
&RAMP ID='burner RAMP', T= 1005 , F= 0.0053 /
&RAMP ID='burner RAMP', T= 1010 , F= 0.0049 /
&RAMP ID='burner RAMP', T= 1015 , F= 0.0049 /
&RAMP ID='burner RAMP', T= 1020 , F= 0.0049 /
&RAMP ID='burner RAMP', T= 1025 , F= 0.0045 /
&RAMP ID='burner RAMP', T= 1030 , F= 0.0045 /
&RAMP ID='burner RAMP', T= 1035 , F= 0.0045 /
&RAMP ID='burner RAMP', T= 1040 , F= 0.0000 /


&ISOF QUANTITY='MIXTURE_FRACTION', VALUE(1)=0.03,VALUE(2)=0.001 /

&OBST XB= 3.60,3.80,  0.00,0.80,  0.00,2.00 /
```

```
&OBST XB= 3.60,3.80,  1.60,2.40,  0.00,2.00 /
&OBST XB= 3.60,3.80,  0.00,3.60,  2.00,2.40 /

&VENT XB= 3.80,6.00,  0.00,0.00,  0.00,2.40, SURF_ID='OPEN' /
&VENT XB= 3.80,6.00,  2.40,2.40,  0.00,2.40, SURF_ID='OPEN' /
&VENT XB= 3.80,6.00,  0.00,3.60,  2.40,2.40, SURF_ID='OPEN' /
&VENT XB= 6.00,6.00,  0.00,2.40,  0.00,2.40, SURF_ID='OPEN' /

&SLCF PBY=1.20, QUANTITY='TEMPERATURE', VECTOR=.TRUE. /

&PL3D DTSAM=2.0, WRITE_XYZ=.TRUE.,
    QUANTITIES='TEMPERATURE', 'U-VELOCITY', 'V-VELOCITY', 'W-VELOCITY', 'PRESSURE' /

&THCP XB=0.00,3.60, 0.00,2.40, 0.00,2.40, QUANTITY='HRR', LABEL='Fire-HRR', DTSAM=2.0 /

&THCP XB=3.70,3.70, 0.80,1.60, 0.00,0.80, QUANTITY='MASS FLOW', LABEL='F-Bo-mf', DTSAM=2.0 /
&THCP XB=3.70,3.70, 0.80,1.60, 0.80,2.00, QUANTITY='MASS FLOW', LABEL='F-Up-mf', DTSAM=2.0 /
&THCP XB=3.70,3.70, 0.80,1.60, 0.00,2.00, QUANTITY='MASS FLOW', LABEL='F-Al-mf', DTSAM=2.0 /

&THCP XYZ=1.80,0.10,2.35, QUANTITY='TEMPERATURE', LABEL='T-a', DTSAM=2.0 /
&THCP XYZ=1.80,2.30,2.35, QUANTITY='TEMPERATURE', LABEL='T-b', DTSAM=2.0 /
&THCP XYZ=2.90,1.20,2.35, QUANTITY='TEMPERATURE', LABEL='T-c', DTSAM=2.0 /

&THCP XYZ=2.90,0.70,2.35, QUANTITY='TEMPERATURE', LABEL='T-d', DTSAM=2.0 /
&THCP XYZ=2.90,0.70,1.95, QUANTITY='TEMPERATURE', LABEL='T-e', DTSAM=2.0 /
&THCP XYZ=2.90,0.70,1.55, QUANTITY='TEMPERATURE', LABEL='T-f', DTSAM=2.0 /
&THCP XYZ=2.90,0.70,1.05, QUANTITY='TEMPERATURE', LABEL='T-g', DTSAM=2.0 /

&THCP XYZ=3.70,1.2,0.10, QUANTITY='TEMPERATURE', LABEL='T-01', DTSAM=2.0 /
&THCP XYZ=3.70,1.2,0.20, QUANTITY='TEMPERATURE', LABEL='T-02', DTSAM=2.0 /
&THCP XYZ=3.70,1.2,0.30, QUANTITY='TEMPERATURE', LABEL='T-03', DTSAM=2.0 /
&THCP XYZ=3.70,1.2,0.40, QUANTITY='TEMPERATURE', LABEL='T-04', DTSAM=2.0 /
&THCP XYZ=3.70,1.2,0.50, QUANTITY='TEMPERATURE', LABEL='T-05', DTSAM=2.0 /
&THCP XYZ=3.70,1.2,0.60, QUANTITY='TEMPERATURE', LABEL='T-06', DTSAM=2.0 /
&THCP XYZ=3.70,1.2,0.70, QUANTITY='TEMPERATURE', LABEL='T-07', DTSAM=2.0 /
&THCP XYZ=3.70,1.2,0.80, QUANTITY='TEMPERATURE', LABEL='T-08', DTSAM=2.0 /
&THCP XYZ=3.70,1.2,0.90, QUANTITY='TEMPERATURE', LABEL='T-09', DTSAM=2.0 /
&THCP XYZ=3.70,1.2,1.00, QUANTITY='TEMPERATURE', LABEL='T-10', DTSAM=2.0 /
&THCP XYZ=3.70,1.2,1.10, QUANTITY='TEMPERATURE', LABEL='T-11', DTSAM=2.0 /
&THCP XYZ=3.70,1.2,1.20, QUANTITY='TEMPERATURE', LABEL='T-12', DTSAM=2.0 /
&THCP XYZ=3.70,1.2,1.30, QUANTITY='TEMPERATURE', LABEL='T-13', DTSAM=2.0 /
&THCP XYZ=3.70,1.2,1.40, QUANTITY='TEMPERATURE', LABEL='T-14', DTSAM=2.0 /
&THCP XYZ=3.70,1.2,1.50, QUANTITY='TEMPERATURE', LABEL='T-15', DTSAM=2.0 /
&THCP XYZ=3.70,1.2,1.60, QUANTITY='TEMPERATURE', LABEL='T-16', DTSAM=2.0 /
&THCP XYZ=3.70,1.2,1.70, QUANTITY='TEMPERATURE', LABEL='T-17', DTSAM=2.0 /
&THCP XYZ=3.70,1.2,1.80, QUANTITY='TEMPERATURE', LABEL='T-18', DTSAM=2.0 /
&THCP XYZ=3.70,1.2,1.90, QUANTITY='TEMPERATURE', LABEL='T-19', DTSAM=2.0 /
&THCP XYZ=3.70,1.2,1.95, QUANTITY='TEMPERATURE', LABEL='T-20', DTSAM=2.0 /
```